Received: 4 July 2021 | Accepted: 2 August 2021
DOI: 10.1111/gcb.15848

PRIMARY RESEARCH ARTICLE

Global Change Biology WILEY

High historical variability weakens the effects of current climate differentiation on microbial community dissimilarity and assembly

Jialiang Kuang[1,2] | **Colin T. Bates**[1] | **Xiaoling Wan**[1,3] | **Daliang Ning**[1] | **Dongmei Deng**[1,4] | **Wensheng Shu**[5] | **Jizhong Zhou**[1,6,7]

[1]Institute for Environmental Genomics and Department of Microbiology and Plant Biology, University of Oklahoma, Norman, Oklahoma, USA

[2]State Key Laboratory of Biocontrol, Guangdong Key Laboratory of Plant Resources and Conservation of Guangdong Higher Education Institutes, College of Ecology and Evolution, Sun Yat-sen University, Guangzhou, China

[3]The Key Laboratory of Aquatic Biodiversity and Conservation of the Chinese Academy of Sciences, Institute of Hydrobiology, Chinese Academy of Sciences, Wuhan, China

[4]Guangxi Key Laboratory of Green Processing of Sugar Resources, College of Biological and Chemical Engineering, Guangxi University of Science and Technology, Liuzhou, China

[5]School of Life Sciences, South China Normal University, Guangzhou, China

[6]Earth Sciences Division, Lawrence Berkeley National Laboratory, Berkeley, California, USA

[7]State Key Joint Laboratory of Environment Simulation and Pollution Control, School of Environment, Tsinghua University, Beijing, China

Correspondence
Jialiang Kuang, Institute for Environmental Genomics and Department of Microbiology and Plant Biology, University of Oklahoma, Norman, OK 73019, USA.
Email: kjialiang@ou.edu

Funding information
National Natural Science Foundation of China, Grant/Award Number: 31600403, 31800422, 31971553, 41622106, 41673111 and U1501232; Natural Science Foundation of Guangdong Province, China, Grant/Award Number: 2016A030312003; National Science Foundation, Grant/Award Number: EF-1065844

Abstract

Understanding the influences of global climate change on soil microbial communities is essential in evaluating the terrestrial biosphere's feedback to this alarming anthropogenic disturbance. However, little is known about how intra-site historical climate variability can mediate the influences of current climate differences on community dissimilarity and assembly. To fill this gap, we examined and disentangled the interactive effects of historical climate variability and current climate differences on the soil bacterial community dissimilarity and stochasticity of community assembly among 143 sites from 28 forests across eastern China. We hypothesize that the relative importance of stochasticity and community dissimilarity are related to historical climate variability and that an increasing sum of intra-site historical variability enhances stochasticity while reduces dissimilarity between two communities. To test our hypothesis, we statistically controlled for covariates between sites including differences in soil chemistry, plant diversity, spatial distance, and seasonal climate variations at annual timescales. We observed that an increase in inter-site current climate differences led to a reduced impact of stochasticity in community assembly and a pronounced divergence between communities. In stark contrast, when communities were subjected to a high level of intra-site historical climate fluctuation, the observed impact incurred from current climate differences was substantially weakened. Moreover, the influence of increased historical variability was consistent along the gradient of current temperature differences between sites. However, effects induced by historical fluctuation in precipitation were disproportional and only evident when small inter-site differences were observed. Consequently, if the prior climate variability is ignored, especially regarding environmental factors like temperature, we assert that the influence current climate differentiation has on regulating community dissimilarity and assembly stochasticity will be underestimated. Together, our findings highlight the importance and need of explicitly controlling the mean and the historical variability of climate factors for the next "generation" of climate change experiments to come.

KEYWORDS
community assembly, community dissimilarity, current climate difference, ecological stochasticity, forest soil, historical climate fluctuation

1 | INTRODUCTION

Evidence is mounting that changes in climate such as warming and water stress influence the structure and functionality of soil bacterial communities (Belay-Tedla et al., 2009; Cregger et al., 2012; Guo et al., 2018, 2019; Ren et al., 2018; Sheik et al., 2011; Zhou et al., 2012, 2016). Our understanding of these effects has been remarkably informed by field studies with experimental climate change treatments. The use of these controlled experimental settings is highly informative in assessing the impacts of climate change. For example, the impact of elevated temperature on the microbial structure and functioning in soils has been examined by a continuous 2–3°C field-based warming treatment (Belay-Tedla et al., 2009; Guo et al., 2018; Sheik et al., 2011; Zhou et al., 2012). However, most of these experiments generally simulate a persistent disturbance and focus on the effects of changes in mean values (i.e., "trend effects") for different climate factors and, as a result, do not explicitly capture the influence of climate variability or extreme events (Jentsch et al., 2007; Thompson et al., 2013). It is projected that the frequency and magnitude of extreme weather events will increase in the near future (Cai et al., 2015; Cohen et al., 2018; Screen & Simmonds, 2014). These extreme weather events change the long-held climate variability patterns globally (Jentsch et al., 2007; Thompson et al., 2013) and could greatly alter the community structure and ecosystem functioning (e.g., composition and secondary production of macroinvertebrates in freshwaters; Ledger et al., 2011). Elucidating the effects of historical climate variability on microbial communities is vital for better estimating its future dynamics and the impacts on ecosystem functions. Therefore, we must advance our understanding of how microbial communities and the relevant assembly processes respond to historical climate variability and its legacy effects (Hawkes & Keitt, 2015), although currently, little is known.

Previous studies of spatial and temporal patterns in climate fluctuations over decades have revealed enormous ecological impacts on terrestrial plant and animal biology through both direct and indirect pathways (Stenseth et al., 2002). Recently, how constraints from prior conditions (i.e., historical contingency) may alter the microbial responses to current environmental changes have attracted a great deal of attention. Increasing evidence demonstrates that the responses of soil respiration (Hawkes et al., 2017), decomposition rate (Martiny et al., 2017), enzyme activity (Averill et al., 2016), microbial growth (de Nijs et al., 2019; Gutknecht et al., 2012), diversity (Ladau et al., 2018), and community composition (Barnard et al., 2015; Evans & Wallenstein, 2012; Evans et al., 2014) are subject to current environmental factors but are shaped by the legacies of past climate conditions. These studies have highlighted that considering the differences in historical environments is essential in predicting future microbial responses under climate change scenarios. Alternatively, there is an increasing awareness of the need for considering the influence of historical climate fluctuations (Hawkes & Keitt, 2015; Thompson et al., 2013), yet relatively little attention has been devoted. In particular, how such historical variability may influence the observed effects of current climate conditions on the differences between communities (i.e., β-diversity) as well as the relative roles of deterministic and stochastic processes (Dini-Andreote et al., 2015; Stegen et al., 2012; Vellend, 2010; Zhou et al., 2014; Zhou & Ning, 2017) in community assembly remains unexplored.

Traditionally, human-induced climate changes such as global warming and drought are considered strong ecological forces that influence microbial diversity and shape community structure (Guo et al., 2018; Sheik et al., 2011; Zhou et al., 2012). When these imposed stresses persistently control and shape the communities with less environmental fluctuations, such abiotic filters tend to impose a strong natural selection on the community, which deterministically drives the community assembly (Ning et al., 2019; Zhou & Ning, 2017). For example, increasing dissimilarities of soil microbial communities between warmed and control samples (with large current climate differences) are found during succession over a long-term effect of warming (i.e., a persistently imposed environmental stress), indicating warming-driven deterministic filtering occurring on microorganisms (Guo et al., 2018). Therefore, a more substantial inter-site difference of current climate conditions (ΔCC; e.g., generated by a natural temperature gradient or a persistent warming treatment) can lead to a decreasing impact of stochasticity in the assembly processes (Figure 1a) and an increasing divergence between communities (Figure 1b).

Microorganisms are generally expected to exhibit resilience to environmental changes because they feature physiological plasticity, dormancy, resuscitation, faster growth and turnover rate, and rapid evolution (Hawkes & Keitt, 2015; Shade et al., 2012). In the face

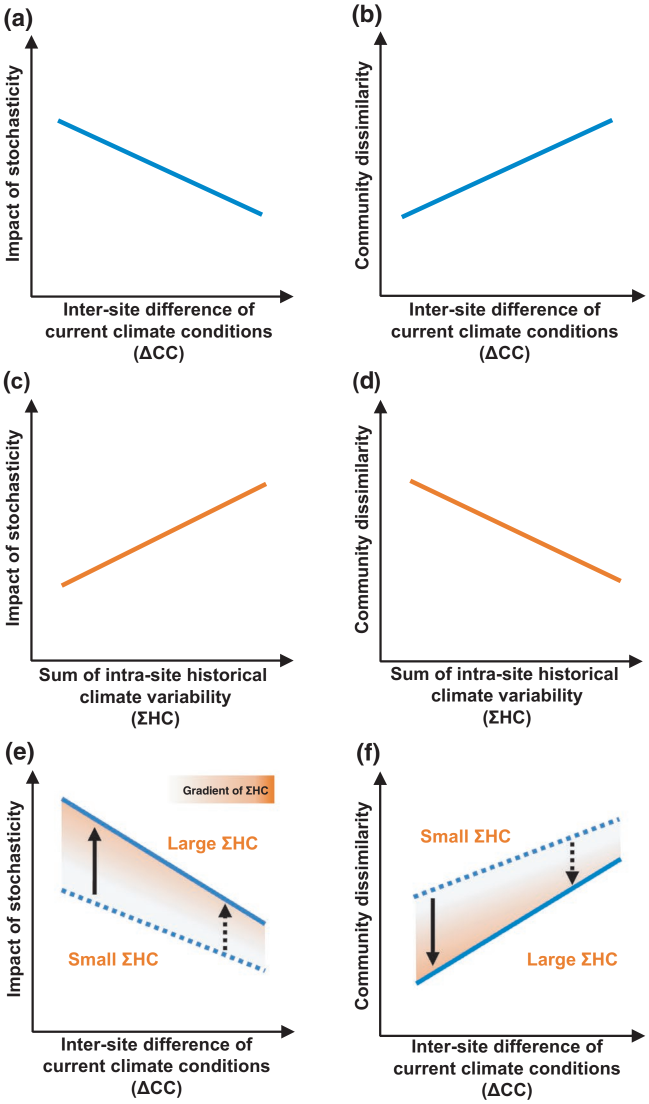

FIGURE 1 Conceptual diagrams showing our hypotheses in this study. We expect that a more substantial inter-site difference of current climate conditions (ΔCC) represents a stronger abiotic environmental stress and deterministically leads to a decreasing impact of stochasticity (a) and an increasing divergence between communities (b). In contrast, when a local community undergoes higher degree of intra-site historical fluctuation, it is expected to suffer more considerable random changes. When a pair of communities are under fluctuated conditions and a larger sum of intra-site historical climate variability (ΣHC) is detected, the impact of stochasticity is expected to be enhanced (c) with less community dissimilarity (d). Due to the opposite effects of ΔCC and ΣHC on the impact of stochasticity and the community dissimilarity, the enhanced ΣHC might weaken the effects of ΔCC, especially when ΔCC is small. Specifically, under the scenarios with an enhanced ΣHC, we expect that the magnitude (i.e., mean) increases for the impact of stochasticity increases (e, solid line) while it decreases for the community dissimilarity (f, solid line) along the gradient of ΔCC. Moreover, the effect of the enhanced ΣHC is expected to be disproportional and more evident when ΔCC is small. Particularly, a larger increase in stochastic impacts (e, solid arrow line) and a greater decrease in the community dissimilarity (f, solid arrow lines) are anticipated under small ΔCC. Moreover, we expected that the observed influence of the enhanced ΣHC would be reduced or may even be negligible (e and f, dashed arrow lines) when the ΔCC is large and provides a stronger and dominant effect than ΣHC [Colour figure can be viewed at wileyonlinelibrary.com]

of shifting conditions, a highly resilient community likely responds quickly and is capable of recovering without qualitatively switching to an alternative stable state (Hawkes & Keitt, 2015; Shade et al., 2012). Nevertheless, in highly fluctuating environments, the resiliency could be largely reduced by historical contingencies, the legacies that can result from the local adaptation and priority effects caused by the previous environmental regime (Shade et al., 2012). As a result, a local community is expected to suffer more considerable random changes when it undergoes a higher degree of intra-site historical fluctuation (e.g., the inter-annual variation of temperature within site).

In terms of the stochastic processes in regulating the community assembly as well as the divergence in community structure between communities, we hypothesize that the relative importance of stochasticity and the community dissimilarity are related to the historical climate variability (HC) of a given pair of communities. Particularly, when a pair of communities are under fluctuated conditions and a larger sum of intra-site historical climate variability (ΣHC) is observed, the impact of stochasticity is expected to be enhanced (Figure 1c) with less community dissimilarity (Figure 1d) than those for community pairs under relatively constant environments (i.e., a smaller ΣHC).

According to this primary hypothesis, ΔCC and ΣHC show opposite effects on the impact of stochasticity and the community dissimilarity (Figure 1a–d). Thus, our second hypothesis is that the effects of ΔCC could be weakened by an enhanced ΣHC, especially when ΔCC is small. Specifically, under the scenarios with an increase in ΣHC, we expect that the magnitude (i.e., mean) increases for the impact of stochasticity (Figure 1e, solid line) while it decreases for the community dissimilarity (Figure 1f, solid line) along the gradient of ΔCC. Furthermore, we expect that the influence of the enhanced ΣHC is disproportional and more substantial when ΔCC is small. Particularly, a larger increase in stochastic impacts (Figure 1e, solid arrow line) and a greater decrease in the community dissimilarity (Figure 1f, solid arrow lines) are anticipated under small ΔCC than those under large ΔCC (Figure 1e,f, dashed arrow lines). Moreover, if the ΔCC is large with a stronger and dominant effect than ΣHC, the observed influence of the enhanced ΣHC would be reduced or may even be negligible (Figure 1e,f, dashed arrow lines).

Here, to test our hypotheses, we present a study ascertaining the effects of ΔCC and ΣHC on the beta-diversity and the relative importance of stochastic/deterministic assembly processes of soil bacterial communities in forest ecosystems. We evaluated the community dissimilarity and the impact of stochasticity (Ning et al., 2019) among the 143 sites in 28 natural forest reserves across eastern China (Figure S1) with a wide range of climate conditions (Chen et al., 2020; Wang et al., 2019). We were particularly interested in how the long-term historical variability could mediate the effects of observed current climate differentiation.

2 | MATERIALS AND METHODS

2.1 | Study sites and soil sampling

We tested our hypotheses using 429 soil samples that were collected from 28 natural forest reserves across a broad range of latitudes (21.88°–53.45°N) and longitudes (100.01°–129.65°E) in eastern China in 2012 (Figure S1; Table S1; Chen et al., 2020; Wang et al., 2019). The soil bacterial communities from these forest ecosystems are shaped by the impacts of a wide gradient of climatic and edaphic conditions.

We collected top layer soils (0–10 cm in depth) from 3 to 14 sites in each forest reserve. The latitude, longitude, and elevation of each site were recorded by a portable GPS machine. The numbers of sites were determined approximately based on the sizes of forest reserves. The locations of sites were selected to represent the gradient of elevation for each forest reserve. In each sampling site, we collected three soil samples as biological replicates that were located ~5 m apart from each other. After the removal of vegetation litter, soils were sampled and stored in sterilized polyethylene bags and kept on ice immediately in the field and then transported to the laboratory.

We performed the measurement of soil properties and the molecular analysis for each biological replicate. In this study, we rarified 9735 bacterial reads for each soil sample (i.e., replicate) and then combined all the reads from the three replicates within each site to generate one composited sample with a total of 29,205 reads (see detailed methods below). Accordingly, the soil properties of each site were estimated as the mean values of the three replicates (see detailed methods below). A few soil samples were discarded because their bags were broken during transportation. Sites without three replicates were then removed from the subsequent analyses. Overall, a total of 429 soil samples were used to represent the soil bacterial communities and soil properties of 143 sites among 28 forest reserves (Figure S1).

2.2 | Soil properties and plant species richness

For each sample (i.e., replicate), soil properties, including moisture, pH, electrical conductivity (EC), total organic carbon (TOC), total nitrogen (TN), total phosphorus (TP), total potassium (TK), as well as available P, K, Al, Ca, and Mg, were measured as described in Wang et al. (2019). The mean values of the three replicates were then calculated for each site (Table S2). For the subsequent analyses, the difference of soil properties between sites was calculated as the pairwise Euclidean distance based on the standardized data of these 12 edaphic variables.

We obtained plant species richness from Wang et al. (2011). In brief, the plant species richness of each forest reserve (Table S2) was determined based on its spatial location and the woody plant distribution map (spatial resolution: 50 × 50 km), which was created by Fang et al. (2011). In this distribution map of woody plant, they compiled the plant species distributions in China from all floras published before 2008, including *Flora of China*, *Higher Plants of China*, *Flora Reipublicae Popularis Sinicae*, more than 120 volumes of provincial floras, and many local floras across China. Moreover, 21 senior botanists from different regions of China were invited to check and supplement the plant species distributions in each region to improve the accuracy of this database. This distribution map matched the survey-based map within 95% confidence (Wang et al., 2012).

2.3 | Climate factors and their historical variability

We downloaded public climate datasets generated by a 194 weather station network spread across China from the National Meteorological Information Center (http://data.cma.cn/en; Figure S2). Although some weather stations have recorded the climate conditions since 1949, the most comprehensive daily records of temperature (°C) and precipitation (mm) from all the stations are available since 1952. Therefore, we extracted these daily records over a 60-year period (1952–2012) to capture the historical climate fluctuations. For temperature, we calculated the monthly means based on the daily data and then averaged the 12 monthly means as the annual mean temperature (AMT) for each year. For precipitation, we summed up the daily data to generate the monthly sums and then added up the 12 monthly sums as the annual precipitation (AP) for each year. We estimated the yearly AMT and AP for each site by applying the kriging interpolation method (Kilibarda et al., 2014) using the "gstat" package in R, and obtained the interpolated AMT and AP according to the site location. By doing this, a total of 61 data points of yearly AMT (or AP) were obtained for each site over the 60-year period.

In addition, we compared the mean annual temperature (MAT) and mean annual precipitation (MAP) that were estimated by the kriging interpolation method against those from historical climate data in "WorldClim" public climate database v2.1 (Fick & Hijmans, 2017). The monthly climate data for mean temperature and precipitation that were corrected by elevation were downloaded at high spatial resolution (30 s, ~1 km^2). Because the historical climate dataset in "WorldClim" was compiled for 1970–2000, the comparison was focused on this period. Monthly values were extracted based on the site locations using the "raster" package in R. For each site, we calculated the AMT and AP of each year and then calculated the MAT and MAP during the period from 1970 to 2000. Accordingly, the MAT and MAP based on datasets using the kriging interpolation method were also calculated for 1970–2000. Consistent patterns of historical climate conditions among our sites were observed between these two datasets with significant correlations (MAT: $r = 0.93$, $p < 0.0001$; MAP: $r = 0.97$, $p < 0.0001$; Pearson correlation; Figure S3). Notably, because sampling sites at a given forest reserve were selected to represent the altitudinal gradient, the macroclimate data from weather stations may not distinguish the local climate differences among sites. Thus, the comparison of sites within the same forest reserve was excluded for the subsequent analyses.

In this study, we used the interpolated data of 2012 (i.e., AMT.2012 and AP.2012) to represent the current climate conditions (CC) of each site (Table S1) and calculated the ΔCC as the pairwise Euclidean distance of standardized values for each climate factor. We also calculated the MAT and MAP over the 60-year period for each site (i.e., MAT.60yrs and MAP.60yrs that were calculated as the means of 61 yearly AMT and AP; Table S1). We found that the AMT and AP of 2012 were strongly and significantly correlated to their long-term averages (AMT.2012 vs. MAT.60yrs: $r = 0.99$, $p < 0.0001$; AP.2012 vs. MAP.60yrs: $r = 0.97$, $p < 0.0001$; Pearson correlation). In addition, we performed Mantel tests to compare the inter-site climate differences (i.e., the pairwise differences among 143 sites) between 2012 and the averages over the 60-year period. The results of Mantel tests further suggested that the ΔCC could indicate the inter-site differentiation in the long-term average effect of environmental stress on the microbial communities (AMT.2012 vs. MAT.60yrs: $r = 0.99$, $p < 0.001$; AP.2012 vs. MAP.60yrs: $r = 0.92$, $p < 0.001$; Mantel test). Therefore, we used the current climate conditions to reflect the natural gradients of annual mean temperature and annual precipitation at the regional scale in this study.

We defined the intra-site historical climate variability (HC) as the coefficient of variation (i.e., a ratio of standard deviation over the mean, CV) of the interpolated values over the 60-year period (i.e., AMT.CV and AP.CV; Table S1). For a given pair of sites, we calculated the ΣHC as the sum of standardized values of the coefficient of variation for each climate factor. In this study, although we mainly focused on the potential effect of historical climate fluctuation on the assembly of soil bacterial communities, the influence of seasonal dynamics of climate conditions at the annual timescale could also alter the microbial communities. Thus, for each site, we calculated the CV of the monthly values of each year and then calculated the mean of 61 CV values over the 60-year period to estimate the intra-site annual climate variation (i.e., TEM.CV and PRE.CV, indicating the means of annual variations of temperature and precipitation, respectively; Table S1).

2.4 | DNA extraction, sequencing, and sequence processing

We extracted the soil microbial DNA from 0.5 g of soil using the MoBio PowerSoil DNA extraction kit following the manufacturer's instructions. To characterized the bacterial communities, we amplified the V4 hypervariable region of the 16S rRNA gene using the 515F (GTGCCAGCMGCCGCGGTAA) and 806R (GGACTACHVGGGTWTCTAAT) primer pair (Chen et al., 2020). We constructed the sequencing libraries by pooling the amplified products from individual soil samples together in equimolar concentrations. After purifying them using the E.Z.N.A.® Gel Extraction Kit, we conducted the sequencing on a 2 × 300 paired-end MiSeq NextGen platform. We processed the raw sequencing data following the UPARSE pipeline (Edgar, 2013). Briefly, we merged the quality-filtered reads into paired-end sequences after deleting the short and low-quality sequences. After removing the chimeric and singleton sequences, we clustered the remaining reads into Operational Taxonomic Units (OTUs) at a 97% similarity threshold. We aligned the representative bacterial OTUs using PASTA (Mirarab et al., 2015) and constructed the phylogenetic tree using FastTree (Price et al., 2010). We rarefied 9735 bacterial reads for each soil sample. All the reads from the three biological replicates were further combined (i.e., a total of 29,205 reads) as a composited sample to represent the community composition of each site. The representative sequences of bacterial OTUs, their abundances in each forest site, and the phylogenetic tree are available in figshare (https://doi.org/10.6084/m9.figshare.12657464).

2.5 | Estimating stochasticity of community assembly

To estimate the relative importance between stochastic and deterministic processes in shaping the bacterial community structure, we calculated the phylogeny-based modified stochasticity ratio (pMST, %) for every pair of sites. The pMST is an index for pairwise comparison and is modified from previous stochasticity ratio indexes (Guo et al., 2018; Ning et al., 2019; Zhou et al., 2014). Briefly, we used the abundance-weighted beta-mean-nearest-taxon-distance (βMNTD) metrics (Stegen et al., 2012) to assess the phylogenetic dissimilarity of bacterial communities between sites. We then calculated the pMST by comparing the observed and null expected phylogenetic beta-diversity as Equations (1) and (2) (Liang et al., 2020). Since the βMNTD has no fixed upper limit, we standardized the βMNTD by dividing it with the estimated maximum βMNTD as previously reported (Ning et al., 2019). Then, we calculated the similarity as the complement, that is, 1 − standardized dissimilarity. The detailed equations were listed below:

$$pMST_{ij} = \frac{\overline{E_{ij}}}{C_{ij}} \bullet \frac{D_{ij}}{\overline{G_{ij}}} \qquad if\ C_{ij} \geq \overline{E_{ij}} \tag{1}$$

$$pMST_{ij} = \frac{\overline{G_{ij}}}{D_{ij}} \bullet \frac{C_{ij}}{\overline{E_{ij}}} \qquad if\ C_{ij} < \overline{E_{ij}} \tag{2}$$

where *Dij* is the observed standardized βMNTD between sites *i* and *j*, *Cij* is the observed similarity, and *Cij* = 1 − *Dij*. $\overline{G_{ij}}$ is the null expectation of standardized βMNTD between sites *i* and *j*, while $\overline{E_{ij}}$ is the null expectation of the similarity. The null communities are generated based on a null model algorithm reported previously (Guo et al., 2018) with 1000 randomization times. For the comparison of stochasticity, a given pair of sites with a higher value of $pMST_{ij}$ suggests that the stochastic processes play relatively more important roles in driving the community turnover than those in other site pairs. The calculation was performed using our in-house pipeline (http://ieg3.rccc.ou.edu:8080/).

2.6 | Statistical analyses

To visualize the temporal fluctuations from 1952 to 2012, we calculated the yearly averages of AMT and AP of sites within each forest reserve along the latitudinal gradient. For each climate factor, we performed the Pearson correlation to relate the historical climate variability to the latitude. For the spatial patterns of historical climate variability across eastern China, the coefficient of variation for each climate factor was interpolated by kriging and visualized on the map.

A total of 9750 data points were used in the statistical analyses, focusing on the differences between any two sites in different forests. Notably, there were 10,153 data points for the complete pairing based on 143 sites, and we excluded 403 data points representing the pairs of sites within the same forest reserve as mentioned above. To test our primary hypothesis, we applied multiple linear regression analysis to explore the relationships relating the ΔCC and ΣHC to the impact of stochasticity (pMST; or the community dissimilarity [weighted UniFrac distance, for convenience, such distance is referred to as UniFrac]). Because our survey was conducted across a large range of biomes and geographic areas, the observed differences in microbial community compositions among sites should also be influenced by a wide variety of soil environmental properties, plant diversities, spatial distances, as well as the seasonal climate variation at the annual timescale. Therefore, for a direct test of the relationships under our historical climate variability model, we calculated the partial effects of ΔCC and ΣHC on the pMST (or UniFrac), holding all other covariates constant.

For this purpose, we regressed the pMST (or UniFrac) on all other covariates using standardized values (Equation 3):

$$y = \gamma_1 \mathrm{SPACE} + \gamma_2 \mathrm{SOIL} + \gamma_3 \mathrm{PLANT} + \gamma_4 \Sigma\mathrm{TEM.CV} + \gamma_5 \Sigma\mathrm{PRE.CV} + \varepsilon \tag{3}$$

where y is the pairwise values of pMST (or UniFrac); SPACE, SOIL, and PLANT are inter-site differences (i.e., Euclidean distances) of geographic locations, soil properties, and plant species richness, respectively; ΣTEM.CV and ΣPRE.CV are the sum of intra-site annual climate variations of temperature and precipitation, respectively. The coefficients γ_s are slopes of the covariates, and ε is the intercept. Similarly, we regressed the ΔCC and ΣHC for each climate factor on these covariates (Equation 4):

$$x = \gamma_1 \mathrm{SPACE} + \gamma_2 \mathrm{SOIL} + \gamma_3 \mathrm{PLANT} + \gamma_4 \Sigma\mathrm{TEM.CV} + \gamma_5 \Sigma\mathrm{PRE.CV} + \varepsilon \tag{4}$$

where x is ΔCC (or ΣHC) of AMT (or AP). We then calculated the residuals from Equation (3) (y_{res}) and Equation (4) (x_{res}), and used these residuals for the subsequent analyses.

Residuals of ΔCC and ΣHC for each climate factor were used in the multiple linear regression models (Equation 5):

$$y_{\mathrm{res}} = a\Delta\mathrm{CC}_{\mathrm{res}} + b\Sigma\mathrm{HC}_{\mathrm{res}} + c \tag{5}$$

where y_{res} is residuals of pMST (or UniFrac), $\Delta\mathrm{CC}_{\mathrm{res}}$ and $\Sigma\mathrm{HC}_{\mathrm{res}}$ are the residuals of ΔCC and ΣHC for AMT (or AP), respectively. The coefficients a and b are slopes of $\Delta\mathrm{CC}_{\mathrm{res}}$ and $\Sigma\mathrm{HC}_{\mathrm{res}}$, respectively, and c is the intercept. We extracted and compared the observed coefficients ($\mathrm{coef}_{\mathrm{obs}}$) of $\Delta\mathrm{CC}_{\mathrm{res}}$ and $\Sigma\mathrm{HC}_{\mathrm{res}}$ to reflect their relative importance in the model. We assessed the significance of the coefficients by a randomization test. Specifically, we randomized the sample labels in the original matrices of $\mathrm{pMST}_{\mathrm{res}}$ (or $\mathrm{UniFrac}_{\mathrm{res}}$) to generate null distance matrices and re-conducted the multiple linear regression analysis. We repeated this randomization 1000 times to form the null distribution of the coefficients. We calculated the *P*-value as the rank of the observed coefficients relative to this null distribution. Meanwhile, the standardized effect size (SES) of the coefficient was calculated as follow (Equation 6):

$$\mathrm{SES.coef} = \left(\mathrm{coef}_{\mathrm{obs}} - \mathrm{coef}_{\mathrm{null}}\right) / \mathrm{SD}_{\mathrm{null}} \tag{6}$$

where $\mathrm{coef}_{\mathrm{obs}}$ is the observed coefficient value, $\mathrm{coef}_{\mathrm{null}}$ is the mean of the simulated values, and $\mathrm{SD}_{\mathrm{null}}$ is the standard deviation of the simulated values. In addition, we performed Mantel and partial Mantel tests to examine the correlations between $\Delta\mathrm{CC}_{\mathrm{res}}$ (or $\Sigma\mathrm{HC}_{\mathrm{res}}$) and $\mathrm{pMST}_{\mathrm{res}}$ (or $\mathrm{UniFrac}_{\mathrm{res}}$).

To test our second hypothesis, we explored how different levels of $\Sigma\mathrm{HC}_{\mathrm{res}}$ could mediate the effect of $\Delta\mathrm{CC}_{\mathrm{res}}$ on the $\mathrm{pMST}_{\mathrm{res}}$ and $\mathrm{UniFrac}_{\mathrm{res}}$ from two angles. First, we expected a considerable difference of $\mathrm{pMST}_{\mathrm{res}}$ (or $\mathrm{UniFrac}_{\mathrm{res}}$) between low and high levels of $\Sigma\mathrm{HC}_{\mathrm{res}}$ along the gradient of $\Delta\mathrm{CC}_{\mathrm{res}}$. Second, if the influence of the enhanced $\Sigma\mathrm{HC}_{\mathrm{res}}$ is more evident when $\Delta\mathrm{CC}_{\mathrm{res}}$ is small, we expected a substantially greater slope of the relationship between $\mathrm{pMST}_{\mathrm{res}}$ (or $\mathrm{UniFrac}_{\mathrm{res}}$) and $\Delta\mathrm{CC}_{\mathrm{res}}$ under a large $\Sigma\mathrm{HC}_{\mathrm{res}}$ than that under a small $\Sigma\mathrm{HC}_{\mathrm{res}}$.

In this study, to better understand the effect of $\Sigma\mathrm{HC}_{\mathrm{res}}$ along the whole gradient of $\Delta\mathrm{CC}_{\mathrm{res}}$, we clustered the whole dataset into two sub-datasets based on different levels of $\Delta\mathrm{CC}_{\mathrm{res}}$ and $\Sigma\mathrm{HC}_{\mathrm{res}}$ for subsequent analyses (Figure S4). Particularly, for each climate factor, we first evenly split the range of $\Delta\mathrm{CC}_{\mathrm{res}}$ into five bins, and divided the values of $\mathrm{pMST}_{\mathrm{res}}$ and $\mathrm{UniFrac}_{\mathrm{res}}$ into five groups accordingly. We then separated each group's values into two sub-groups based on the group's median of $\Sigma\mathrm{HC}_{\mathrm{res}}$. By doing so, the level of $\Delta\mathrm{CC}_{\mathrm{res}}$ between the two sub-groups remained similar while the differentiation in $\Sigma\mathrm{HC}_{\mathrm{res}}$ was maximized. We combined all the sub-groups under small or large $\Sigma\mathrm{HC}_{\mathrm{res}}$ (i.e., low or high levels of $\Sigma\mathrm{HC}_{\mathrm{res}}$ according to the group's median), respectively, to generate two sub-datasets with a similar range of $\Delta\mathrm{CC}_{\mathrm{res}}$ but an apparent difference in $\Sigma\mathrm{HC}_{\mathrm{res}}$. To test whether this arbitrary clustering may influence the results, we repeated this procedure to form different pairs of sub-datasets by evenly splitting the range of $\Delta\mathrm{CC}_{\mathrm{res}}$ into 10, 15, and 20 bins, respectively and re-conducted the subsequent analyses. The raw data in terms of the clustering of subsets based on low and high levels of $\Sigma\mathrm{HC}_{\mathrm{res}}$ across different ranges of $\Delta\mathrm{CC}_{\mathrm{res}}$ (i.e., 5, 10, 15, 20 bins) are available in figshare (https://doi.org/10.6084/m9.figshare.12657464).

We evaluated the difference of $\mathrm{pMST}_{\mathrm{res}}$ (or $\mathrm{UniFrac}_{\mathrm{res}}$) between a given pair of sub-datasets by the Wilcoxon rank-sum test. In

TABLE 1 Summary of statistics of multiple linear regression

Climate factors	Variables	Stochasticity ($pMST_{res}$) coef$_{obs}$	*p*-value	SES.coef	Community dissimilarity ($UniFrac_{res}$) coef$_{obs}$	*p*-value	SES.coef
AMT	ΔCC_{res}	−0.014	0.078	−1.325	0.013	0.125	0.994
	ΣHC_{res}	0.027	<0.001	2.792	−0.028	<0.001	−3.549
AP	ΔCC_{res}	−0.068	<0.001	−11.606	0.049	<0.001	8.945
	ΣHC_{res}	−0.016	0.075	−1.422	−0.002	0.294	−0.516

Note: Residuals of ΔCC and ΣHC for each climate factor were used in the multiple linear regression models ($y_{res} \sim a\Delta CC_{res} + b\Sigma HC_{res} + c$). The coefficients (i.e., slopes) were extracted from the models and their significance (*p*-value) were determined by the randomization test (1000 times). The standardized effect size (SES) of the coefficient was calculated as: SES.coef = (coef$_{obs}$ − coef$_{null}$)/SD$_{null}$. $pMST_{res}$: residuals of the impact of stochasticity; $UniFrac_{res}$: residuals of the weighted UniFrac distance; ΔCC_{res}: residuals of the inter-site difference of current climate conditions; ΣHC_{res}: residuals of the sum of intra-site historical climate variability.

Abbreviations: AMT, annual mean temperature; AP, annual precipitation.

TABLE 2 Mantel and partial Mantel tests for the correlations linking the residuals of stochasticity (or community dissimilarity) to ΔCC_{res} and ΣHC_{res}

Effects of	Controlling for	Stochasticity ($pMST_{res}$) AMT	Stochasticity ($pMST_{res}$) AP	Community dissimilarity ($UniFrac_{res}$) AMT	Community dissimilarity ($UniFrac_{res}$) AP
ΔCC_{res}		−0.041	-0.370^{***}	−0.001	0.277^{***}
ΣHC_{res}		0.108^{*}	-0.174^{**}	-0.151^{***}	0.099^{*}
ΔCC_{res}	ΣHC_{res}	−0.074	-0.337^{***}	0.043	0.260^{***}
ΣHC_{res}	ΔCC_{res}	0.125^{**}	−0.067	-0.157^{***}	0.014

Note: Tests were conducted using Pearson's *r* for different climate factors. The significances were tested based on 999 permutations.

***$p < 0.001$; **$p < 0.01$; *$p < 0.05$.

addition, we calculated the effect size for this Wilcoxon rank-sum test using the "rstatix" package in R to estimate the magnitude of differences between the sub-datasets under small and large ΣHC_{res}. The *r* values of the Wilcoxon effect size (Wilcox.effs *r*) were calculated as follow (Equation 7):

$$r = Z/\sqrt{n} \tag{7}$$

where *Z* is the *Z* statistic for the Wilcoxon rank-sum test and *n* is the sum of observations in both groups. The *r* value of Wilcox.effs varies from 0 to close to 1, and is used to define the magnitude of differences, including "negligible" ($r < 0.1$), "small" ($0.1 \le r < 0.3$), "moderate" ($0.3 \le r < 0.5$), and "large" ($r \ge 0.5$).

Moreover, for a given pair of sub-datasets, we performed a simple linear model analysis to correlate $pMST_{res}$ (or $UniFrac_{res}$) and ΔCC_{res} and calculated the coef$_{obs}$. We further calculated the difference of coef$_{obs}$ (Δcoef) between sub-datasets under small and large ΣHC_{res} (Δcoef = coef$_{small \cdot \Sigma HCres}$ − coef$_{large.\Sigma HCres}$). The significance of Δcoef was also estimated by a randomization test (1000 times). We clustered each randomized dataset into two null sub-datasets, as mentioned above, and generated the null distribution of Δcoef. The SES.Δcoef was also calculated. The Δcoef, as well as the averages of $pMST_{res}$ (or $UniFrac_{res}$), were used to examine whether the influence of an enhanced ΣHC_{res} might be disproportional along the gradient of ΔCC_{res}.

3 | RESULTS

3.1 | Current condition and historical variability of climate factors

The 143 sites from the 28 natural forest reserves were characterized by a wide variety of mean annual temperature (MAT.60yrs, 11.9 ± 7.1°C) and mean annual precipitation (MAP.60yrs, 1069.67 ± 561.4 mm) over the period from 1952 to 2012 (Table S1). We observed a consistent trend in the yearly AMT and AP among the different forest reserves along the latitude over the 60-year period (Figure S5). Generally, our results indicated an increasing AMT and a decreasing AP in eastern China over time. In addition, both AMT and AP decreased with increasing latitude (Figure S5). Furthermore, we found space-dependent patterns of historical variability over a half-century of climate change (Figure S6), and the CV values were positively and significantly related to the latitude (Pearson's *r*, 0.65/0.71, AMT.CV/AP.CV, $p < 0.001$).

3.2 | Opposite effects between ΔCC and ΣHC

Significant relationships ($p < 0.05$, randomization test) were found in the results of multiple linear regression, showing that the values of ΔCC_{res} of AP were negatively related to $pMST_{res}$ (coef$_{obs}$: −0.068) while positively related to $\text{UniFrac}_{\text{res}}$ (coef_{obs}: 0.049; Table 1). However, the values of $\Delta\text{CC}_{\text{res}}$ of AMT were not significantly related to pMST_{res} or $\text{UniFrac}_{\text{res}}$. In contrast, we observed a significant and positive relationship between $\Sigma\text{HC}_{\text{res}}$ of AMT and pMST_{res} (coef_{obs}: 0.027) but a negative correlation between $\Sigma\text{HC}_{\text{res}}$ of AMT and $\text{UniFrac}_{\text{res}}$ (coef_{obs}: −0.028). Nevertheless, there were no significant relationships between $\Sigma\text{HC}_{\text{res}}$ of AP and pMST_{res} (or $\text{UniFrac}_{\text{res}}$). Consistent patterns were shown in the results of the Mantel and partial Mantel tests (Table 2). By accounting for the interactions between $\Delta\text{CC}_{\text{res}}$ and $\Sigma\text{HC}_{\text{res}}$, we observed that the $\Delta\text{CC}_{\text{res}}$ of AP and the $\Sigma\text{HC}_{\text{res}}$ of AMT were significantly (positively or negatively) related to pMST_{res} and $\text{UniFrac}_{\text{res}}$ after controlling for the effects of $\Sigma\text{HC}_{\text{res}}$ (or $\Delta\text{CC}_{\text{res}}$; Table 2). In general, these results supported our primary hypothesis that ΣHC shows opposite effects compared to ΔCC, and the increase in ΣHC promotes the relative importance of stochasticity in assembly processes and reduces the divergence in community structure.

By comparing the degrees of SES.coef in multiple linear regression models as well as the Pearson's *r* in partial Mantel tests (Tables 1 and 2), we found that the effects of $\Delta\text{CC}_{\text{res}}$ of AMT were much weaker than those of $\Delta\text{CC}_{\text{res}}$ of AP. Inversely, the $\Sigma\text{HC}_{\text{res}}$ of AMT provided a more considerable impact than those of $\Sigma\text{HC}_{\text{res}}$ of AP, highlighting the importance of historical variability of temperature in community assembly.

3.3 | Influence of different levels of ΣHC on the effects of ΔCC

In general, compared to the results from a low level of $\Sigma\text{HC}_{\text{res}}$, the values of pMST_{res} were significantly ($p < 0.001$, Wilcoxon rank-sum test) greater under a high level of $\Sigma\text{HC}_{\text{res}}$ along the range of $\Delta\text{CC}_{\text{res}}$ for both AMT and AP (Figure 2a,b; Table S3). A total of 9750 data points were used in the analyses and the numbers of data points in each bin were shown in Table S3). In contrast, we found significant ($p < 0.001$) decrease in values of $\text{UniFrac}_{\text{res}}$ when the $\Sigma\text{HC}_{\text{res}}$ increased (Figure 2c,d; Table S3). Together, these results suggested that the increase in ΣHC could weaken the effects of ΔCC on the assembly stochasticity and community dissimilarity. However, the magnitude of this alleviation was larger for temperature than precipitation, revealed by greater degrees between effect sizes (pMST_{res}: 0.147 vs. 0.062; $\text{UniFrac}_{\text{res}}$: 0.142 vs. 0.098, Wilcox.effs *r*; Figure 2; Table S3).

To examine whether the high level of ΣHC had disproportional influence along the gradient of ΔCC, we compared the coefficients of relationships relating $\Delta\text{CC}_{\text{res}}$ to pMST_{res} (or $\text{UniFrac}_{\text{res}}$) under small and large $\Sigma\text{HC}_{\text{res}}$. For the relationships between $\Delta\text{CC}_{\text{res}}$ of AMT and pMST_{res} (or $\text{UniFrac}_{\text{res}}$), we observed similar trends showing that the Δcoef was non-significant (pMST_{res}: $p = 0.311$; $\text{UniFrac}_{\text{res}}$: $p = 0.193$; randomization test) with a relatively small effect size (pMST_{res}: SES.Δcoef = −0.487; $\text{UniFrac}_{\text{res}}$: SES.Δcoef = −0.880; Figure 3a,c; Table S4). However, we found that the influences of high level of $\Sigma\text{HC}_{\text{res}}$ were considerable and were of similar magnitude under small and large $\Delta\text{CC}_{\text{res}}$ of AMT (pMST_{res}: 0.166/0.167; $\text{UniFrac}_{\text{res}}$: 0.121/0.192; Wilcox.effs *r*; Figures S7a,c). These results indicated that the enhanced ΣHC of AMT imposed a consistent impact that leads to an increase in pMST and a decrease in the UniFrac along the gradient of ΔCC.

In contrast, for the correlations between $\Delta\text{CC}_{\text{res}}$ of AP and pMST_{res} (or $\text{UniFrac}_{\text{res}}$), we found a significant ($p < 0.001$; randomization test) difference of coefficients between low and high levels of $\Sigma\text{HC}_{\text{res}}$ with much greater effect sizes than those for AMT (pMST_{res}: SES.Δcoef = 3.094; $\text{UniFrac}_{\text{res}}$: SES.Δcoef = −3.796; Figure 3b,d; Table S4). The changes in slope for these correlations suggested a disproportional influence of high level of ΣHC along the gradient of ΔCC. A large differentiation in effect size was observed between small and large $\Delta\text{CC}_{\text{res}}$ of AP (Figures S7b,d), revealing that the influence of high level of $\Sigma\text{HC}_{\text{res}}$ was only considerable under small $\Delta\text{CC}_{\text{res}}$ of AP (pMST_{res}: Wilcox.effs $r = 0.219$; $\text{UniFrac}_{\text{res}}$: Wilcox.effs $r = 0.203$), yet it could be negligible when the $\Delta\text{CC}_{\text{res}}$ was large (pMST_{res}: Wilcox.effs $r = 0.083$; $\text{UniFrac}_{\text{res}}$: Wilcox.effs $r = 0.009$). These patterns were in line with the results of regression models and partial Mantel tests, showing that the influence of ΔCC was much stronger than that of ΣHC for AP. In general, results for AP supported our second hypothesis, suggesting that the effect of the high level of ΣHC was disproportional and the observed impact of ΔCC could be more substantially alleviated, especially when the ΔCC is small.

4 | DISCUSSION

As one of the major human impacts, globally pervasive climate change not only results in a gradual shift of mean annual climate values but also changes the frequency and severity of extreme events (IPCC, 2013) and fundamentally alters the inherent natural variability of different climate conditions (Seneviratne et al., 2012). Concerns about the increasing climate variability have been widely acknowledged and raised due to its critical consequences on diverse ecosystems (Frank et al., 2015). Intensive studies have indicated that global climate change has an undoubted impact on the microbial community structure and influences the microbially mediated ecosystem C and N cycling (Bardgett et al., 2008; Diamond et al., 2019; Frey et al., 2013; Glassman et al., 2018; Kirchman et al., 2009; Li et al., 2019; Nielsen & Ball, 2015; Zhou et al., 2012). Instead of addressing the importance of average changes, we have concentrated on how historical variability over a half-century could mediate the observed influence of current climate differentiation on community dissimilarity and assembly. Our findings are in line with our primary hypothesis and have revealed that the increase in historical climate variability could promote the impact of stochasticity yet reduce the divergence between local soil bacterial communities in forest ecosystems.

Our findings have partly supported our second hypothesis that the enhanced historical climate variability provides contrary effects to weaken the observed influence of current climate difference on the impact of stochasticity and community dissimilarity. Such

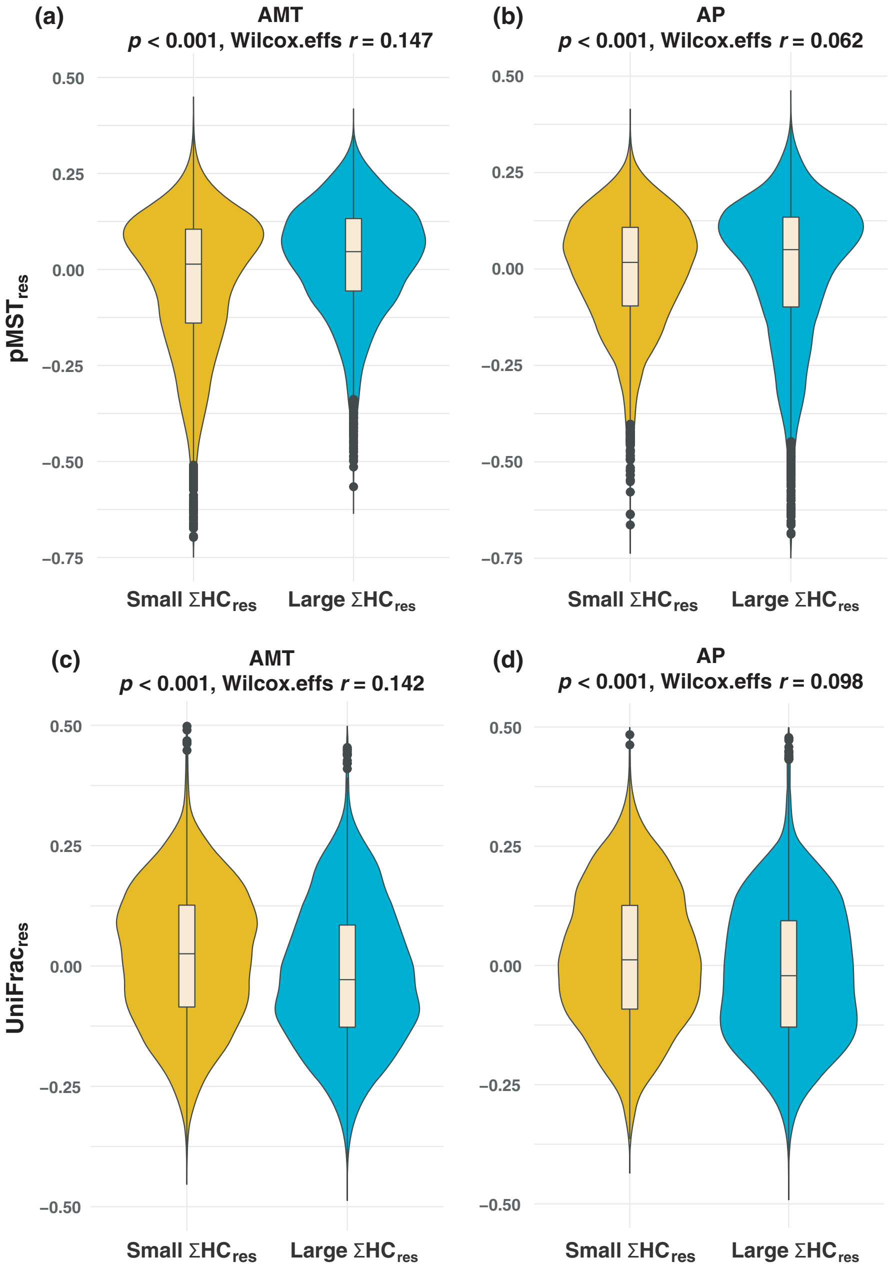

FIGURE 2 Comparison of $\mathrm{pMST_{res}}$ (a, b) and $\mathrm{UniFrac_{res}}$ (c, d) between low and high levels of $\Sigma\mathrm{HC_{res}}$ with a similar range of $\Delta\mathrm{CC_{res}}$. To estimate the influence of different levels of $\Sigma\mathrm{HC_{res}}$ on the effects of $\Delta\mathrm{CC_{res}}$, the range of $\Delta\mathrm{CC_{res}}$ for each climate factor was evenly split into five bins and the values of $\mathrm{pMST_{res}}$ and $\mathrm{UniFrac_{res}}$ were then divided into five groups accordingly (see Figure S4). The values of each group were separated into two sub-groups based on the group's median of $\Sigma\mathrm{HC_{res}}$. All the sub-groups under small or large $\Sigma\mathrm{HC_{res}}$ (i.e., low or high levels of $\Sigma\mathrm{HC_{res}}$ according to the group's median) were finally combined, respectively, to generate two sub-datasets with a similar range of $\Delta\mathrm{CC_{res}}$ but an apparent difference in $\Sigma\mathrm{HC_{res}}$. The significance (p-value) of differences in $\mathrm{pMST_{res}}$ (or $\mathrm{UniFrac_{res}}$) between small and large $\Sigma\mathrm{HC_{res}}$ was estimated by the Wilcoxon rank-sum test. The magnitude of difference was also evaluated by the effect size for the Wilcoxon rank-sum test (Wilcox.effs r), including "negligible" ($r < 0.1$), "small" ($0.1 \le r < 0.3$), "moderate" ($0.3 \le r < 0.5$), and "large" ($r \ge 0.5$). $\mathrm{pMST_{res}}$: residuals of the impact of stochasticity; $\mathrm{UniFrac_{res}}$: residuals of the weighted UniFrac distance; $\Delta\mathrm{CC_{res}}$: residuals of the inter-site difference of current climate conditions; $\Sigma\mathrm{HC_{res}}$: residuals of the sum of intra-site historical climate variability. See details of residual calculation in Section 2 [Colour figure can be viewed at wileyonlinelibrary.com]

effect is expected to be disproportional and could be overridden by stronger selective stresses from greater differentiation in current climate conditions. However, only the patterns for precipitation follow this hypothesis, and the alleviation is unexpectedly consistent along the gradient of current temperature differences. We have further tested our hypotheses based on the rare biosphere, since these sub-communities are increasingly recognized to harbor keystone taxa and have an over-proportional role in biogeochemical cycles and microbiome function (Banerjee et al., 2018; Jousset et al., 2017). Our primary hypothesis is well supported when considering the sub-communities of rare OTUs (i.e., those OTUs with less than 0.1% of relative abundances across all the 143 sampling sites, representing 15.04 ± 4.77% of the total communities; Tables S5 and S6). Interestingly, we found that the enhanced historical variability of both temperature and precipitation can consistently weaken the observed influence of current climate difference (Table S7 and S8), revealing a significant impact on the assembly of rare taxa. Compared to the abundant species, these rare populations are relatively low in abundance and are more likely governed by ecological drift due to the inherent random processes of birth, death, and reproduction (Nemergut et al., 2013; Zhou & Ning, 2017). These findings imply that the rare taxa might be more susceptible to the dramatic changing scenarios and the influences by the impact of stochastic processes rather than abundant ones. Given that this rare biosphere is crucial in promoting long-term ecosystem resilience and ecological stability (Lynch & Neufeld, 2015), our findings suggest that historical climate variability could be one of the major factors controlling the assembly of rare species over spatiotemporal scales, which enabling prospective predictions of ecosystem responses (Jia et al., 2018).

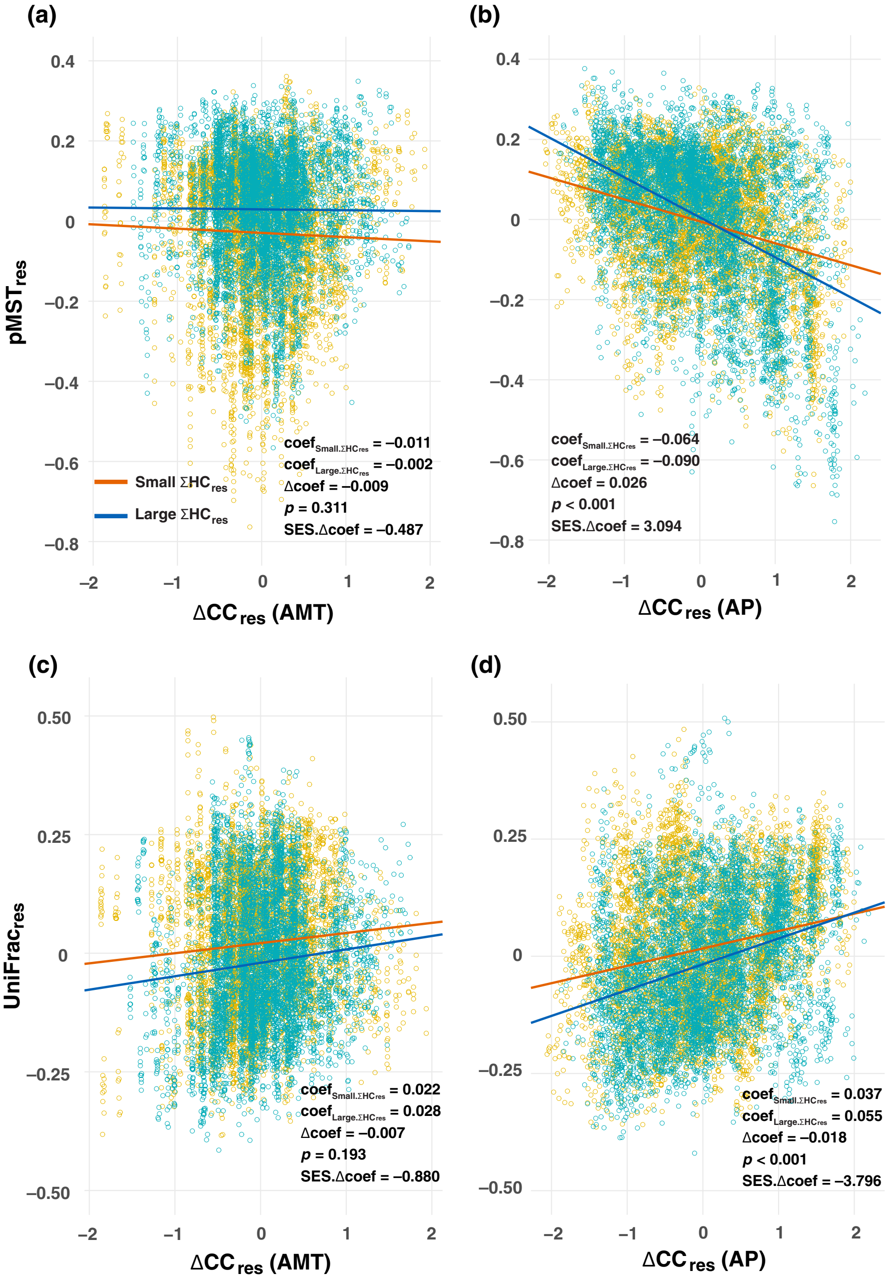

FIGURE 3 Comparison of coefficients of the relationships relating ΔCC_{res} to $pMST_{res}$ (a, b) or $UniFrac_{res}$ (c, d) under low and high levels of ΣHC_{res}. The generation of the two observed (or null) sub-datasets with small and large ΣHC_{res} was described in Figure 2 and Figure S4. Specifically, a total of 9750 data points were used in this analysis. The numbers of data points in different bins are shown in Table S4. The low and high levels of ΣHC_{res} were defined according to the median of each bin. The significance (p-value) of Δcoef ($coef_{Small.\Sigma HCres} - coef_{Large.\Sigma HCres}$) and the standardized effect size (SES) of Δcoef (($\Delta coef_{obs} - \Delta coef_{null})/SD_{null}$) between sub-datasets were calculated by randomization test (1000 times). $pMST_{res}$: residuals of the impact of stochasticity; $UniFrac_{res}$: residuals of the weighted UniFrac distance; ΔCC_{res}: residuals of the inter-site difference of current climate conditions; ΣHC_{res}: residuals of the sum of intra-site historical climate variability. See details of residual calculation in Section 2 [Colour figure can be viewed at wileyonlinelibrary.com]

The distinct results we observed between climate factors and sub-communities may associate with the differences in response and tolerance of microbial communities to the changes in precipitation and temperature as well as the legacy effects under different perturbation patterns over a long-term period. Although the influence of different historical climate conditions on soil microbial communities has been widely addressed (Averill et al., 2016; Barnard et al., 2015; Evans & Wallenstein, 2012; Evans et al., 2014; Gutknecht et al., 2012; Hawkes & Keitt, 2015; Hawkes et al., 2017; Ladau et al., 2018; Martiny et al., 2017), comprehensive research considering the long-term variability of both warming and water stress (Rousk et al., 2013) and their effects on different microbial sub-communities is relatively limited, requiring further study. In summary, this study has highlighted the importance of empirical time-series studies with new "generation" of climate change experiments (Thompson et al., 2013) via explicitly controlling the mean and the variability of climate factors across diverse ecosystems.

Seasonal trajectories of community turnover are commonly detected in diverse ecosystems, resulting from different community responses to the shifting environments and disturbances (Shade et al., 2012). These short-term changes include a large number of unpredictable disturbance events, which can influence the biological interactions, community compositions, and assembly processes (Fuhrman et al., 2015; Zhou & Ning, 2017), and be captured by the temporal changes of rare microorganisms (Shade et al., 2014). In this study, we have considered the average annual variations of the climate conditions over decades (i.e., TEM.CV and PRE.CV) as covariates and statistically controlled them in our historical climate variability model. Nevertheless, we acknowledge that the seasonal/annual dynamics of community composition and its influence on the effect of long-term historical climate variability remain unclear. Thus, distinguishing the differentiation of short-term (e.g., weekly/seasonal) and long-term (e.g., interannual) changes in community structure and assembly processes are required in the future to validate the effects observed in this study.

Understanding how soil bacteria fulfill multiple important biogeochemical functions in forest ecosystems has advanced in recent years, whereas model-based predictions of how their responses to global climate change influence such ecosystem functions are far from completed (Lladó et al., 2017). This great challenge is mainly due to the temporal lags in microbial responses and the uncertain changes in community assembly caused by past climate events (Averill et al., 2016; Hawkes & Keitt, 2015; Hawkes et al., 2017). More empirical and theoretical studies exploring the differentiations in local adaptation and vulnerability to disturbance among diverse microorganisms (e.g., generalists/specialists) (Mariadassou et al., 2015; Slatyer et al., 2013) as well as the microbial dormancy and resuscitation in the face of environmental changes (Jones & Lennon, 2010; Lennon & Jones, 2011) may help to unveil the underlying mechanisms. Together, considering the spatial pattern of ongoing climate variability may improve our ability to simulate the dynamics of large-scale biogeochemical cycles under future global change scenarios.

ACKNOWLEDGEMENTS

Funding for this study was provided by National Natural Science Foundation of China (No. 31600403, 31800422, 41673111, U1501232, 41622106, and 31971553), Natural Science Foundation of Guangdong Province, China (No. 2016A030312003), and the U.S. National Science Foundation MacroSystems Biology program under the contract (NSF EF-1065844).

CONFLICT OF INTEREST

The authors declare no competing interests.

AUTHORS' CONTRIBUTIONS

All authors contributed to the intellectual development of this study. J.K., W.S., and J.Z. conceived the research. J.K. and D.N. constructed the conceptual framework. J.K., D.N., X.W., and D.D. performed the data analyses and statistics. J.K. and C.T.B. drafted the manuscript with help from D.N., W.S., and J.Z.

DATA AVAILABILITY STATEMENT

The representative sequences of bacterial OTUs, their abundances in each forest site, and the phylogenetic tree have been deposited in figshare (https://doi.org/10.6084/m9.figshare.12657464).

ORCID

Jialiang Kuang https://orcid.org/0000-0001-9492-6151
Colin T. Bates https://orcid.org/0000-0002-1468-818X
Daliang Ning https://orcid.org/0000-0002-3368-5988

REFERENCES

Averill, C., Waring, B. G., & Hawkes, C. V. (2016). Historical precipitation predictably alters the shape and magnitude of microbial functional response to soil moisture. *Global Change Biology*, *22*, 1957–1964. https://doi.org/10.1111/gcb.13219

Banerjee, S., Schlaeppi, K., & van der Heijden, M. G. (2018). Keystone taxa as drivers of microbiome structure and functioning. *Nature Reviews Microbiology*, *16*, 567–576. https://doi.org/10.1038/s41579-018-0024-1

Bardgett, R. D., Freeman, C., & Ostle, N. J. (2008). Microbial contributions to climate change through carbon cycle feedbacks. *The ISME Journal*, *2*, 805–814. https://doi.org/10.1038/ismej.2008.58

Barnard, R. L., Osborne, C. A., & Firestone, M. K. (2015). Changing precipitation pattern alters soil microbial community response to wet-up under a Mediterranean-type climate. *The ISME Journal*, *9*, 946–957. https://doi.org/10.1038/ismej.2014.192

Belay-Tedla, A., Zhou, X., Su, B., Wan, S., & Luo, Y. (2009). Labile, recalcitrant, and microbial carbon and nitrogen pools of a tallgrass prairie soil in the US Great Plains subjected to experimental warming and clipping. *Soil Biology and Biochemistry*, *41*, 110–116. https://doi.org/10.1016/j.soilbio.2008.10.003

Cai, W., Wang, G., Santoso, A., McPhaden, M. J., Wu, L., Jin, F. F., Timmermann, A., Collins, M., Vecchi, G., Lengaigne, M., England, M. H., Dommenget, D., Ken, T., & Guilyardi, E. (2015). Increased frequency of extreme La Niña events under greenhouse warming. *Nature Climate Change*, *5*, 132–137. https://doi.org/10.1038/nclimate2492

Chen, Y., Kuang, J., Wang, P., Shu, W., & Barberán, A. (2020). Associations between human impacts and forest soil microbial communities. *Elementa: Science of the Anthropocene*, *8*, 005. https://doi.org/10.1525/elementa.005

Cohen, J., Pfeiffer, K., & Francis, J. A. (2018). Warm Arctic episodes linked with increased frequency of extreme winter weather in the United States. *Nature Communications*, *9*, 869. https://doi.org/10.1038/s41467-018-02992-9

Cregger, M. A., Schadt, C. W., McDowell, N. G., Pockman, W. T., & Classen, A. T. (2012). Response of the soil microbial community to changes in precipitation in a semiarid ecosystem. *Applied and Environmental Microbiology*, *78*, 8587–8594. https://doi.org/10.1128/AEM.02050-12

de Nijs, E. A., Hicks, L. C., Leizeaga, A., Tietema, A., & Rousk, J. (2019). Soil microbial moisture dependences and responses to drying–rewetting: The legacy of 18 years drought. *Global Change Biology*, *25*, 1005–1015. https://doi.org/10.1111/gcb.14508

Diamond, S., Andeer, P. F., Li, Z., Crits-Christoph, A., Burstein, D., Anantharaman, K., Lane, K. R., Thomas, B. C., Pan, C., Northen, T. R., & Banfield, J. F. (2019). Mediterranean grassland soil C-N compound turnover is dependent on rainfall and depth, and is mediated by genomically divergent microorganisms. *Nature Microbiology*, *4*, 1356–1367. https://doi.org/10.1038/s41564-019-0449-y

Dini-Andreote, F., Stegen, J. C., Van Elsas, J. D., & Salles, J. F. (2015). Disentangling mechanisms that mediate the balance between stochastic and deterministic processes in microbial succession. *Proceedings of the National Academy of Sciences of the United States of America*, *112*, E1326–E1332. https://doi.org/10.1073/pnas.1414261112

Edgar, R. C. (2013). UPARSE: Highly accurate OTU sequences from microbial amplicon reads. *Nature Methods*, *10*, 996–998. https://doi.org/10.1038/nmeth.2604

Evans, S. E., & Wallenstein, M. D. (2012). Soil microbial community response to drying and rewetting stress: Does historical precipitation regime matter? *Biogeochemistry*, *109*, 101–116. https://doi.org/10.1007/s10533-011-9638-3

Evans, S. E., Wallenstein, M. D., & Burke, I. C. (2014). Is bacterial moisture niche a good predictor of shifts in community composition under long-term drought? *Ecology*, *95*, 110–122. https://doi.org/10.1890/13-0500.1

Fang, J. Y., Wang, Z. H., & Tang, Z. Y. (2011). *Atlas of woody plants in China: Distribution and climate*. Springer Science & Business Media.

Fick, S. E., & Hijmans, R. J. (2017). WorldClim 2: New 1-km spatial resolution climate surfaces for global land areas. *International Journal of Climatology*, *37*, 4302–4315. https://doi.org/10.1002/joc.5086

Frank, D., Reichstein, M., Bahn, M., Thonicke, K., Frank, D., Mahecha, M. D., Smith, P., van der Velde, M., Vicca, S., Babst, F., Beer, C., Buchmann, N., Canadell, J. G., Ciais, P., Cramer, W., Ibrom, A., Miglietta, F., Poulter, B., Rammig, A., … Zscheischler, J. (2015). Effects of climate extremes on the terrestrial carbon cycle: Concepts, processes and potential future impacts. *Global Change Biology*, *21*, 2861–2880. https://doi.org/10.1111/gcb.12916

Frey, S. D., Lee, J., Melillo, J. M., & Six, J. (2013). The temperature response of soil microbial efficiency and its feedback to climate. *Nature Climate Change*, *3*, 395–398. https://doi.org/10.1038/nclimate1796

Fuhrman, J. A., Cram, J. A., & Needham, D. M. (2015). Marine microbial community dynamics and their ecological interpretation. *Nature Reviews Microbiology*, *13*, 133–146. https://doi.org/10.1038/nrmicro3417

Glassman, S. I., Weihe, C., Li, J., Albright, M. B., Looby, C. I., Martiny, A. C., Treseder, K. K., Allison, S. D., & Martiny, J. B. (2018). Decomposition responses to climate depend on microbial community composition. *Proceedings of the National Academy of Sciences of the United States of America*, *115*, 11994–11999. https://doi.org/10.1073/pnas.1811269115

Guo, X., Feng, J., Shi, Z., Zhou, X., Yuan, M., Tao, X., Hale, L., Yuan, T., Wang, J., Qin, Y., Zhou, A., Fu, Y., Wu, L., He, Z., Van Nostrand, J. D., Ning, D., Liu, X., Luo, Y., Tiedje, J. M., … Zhou, J. (2018). Climate warming leads to divergent succession of grassland microbial communities. *Nature Climate Change*, *8*, 813–818. https://doi.org/10.1038/s41558-018-0254-2

Guo, X., Zhou, X., Hale, L., Yuan, M., Ning, D., Feng, J., Shi, Z., Li, Z., Feng, B., Gao, Q., Wu, L., Shi, W., Zhou, A., Fu, Y., Wu, L., He, Z., Van Nostrand, J. D., Qiu, G., Liu, X., … Zhou, J. (2019). Climate warming accelerates temporal scaling of grassland soil microbial biodiversity. *Nature Ecology & Evolution*, *3*, 612–619. https://doi.org/10.1038/s41559-019-0848-8

Gutknecht, J. L., Field, C. B., & Balser, T. C. (2012). Microbial communities and their responses to simulated global change fluctuate greatly over multiple years. *Global Change Biology*, *18*, 2256–2269. https://doi.org/10.1111/j.1365-2486.2012.02686.x

Hawkes, C. V., & Keitt, T. H. (2015). Resilience vs. historical contingency in microbial responses to environmental change. *Ecology Letters*, *18*, 612–625. https://doi.org/10.1111/ele.12451

Hawkes, C. V., Waring, B. G., Rocca, J. D., & Kivlin, S. N. (2017). Historical climate controls soil respiration responses to current soil moisture. *Proceedings of the National Academy of Sciences of the United States of America*, *114*, 6322–6327. https://doi.org/10.1073/pnas.1620811114

IPCC. (2013). *Working group I contribution to the IPCC fifth assessment report, climate change 2013: The physical science basis*. IPCC.

Jentsch, A., Kreyling, J., & Beierkuhnlein, C. (2007). A new generation of climate-change experiments: Events, not trends. *Frontiers in Ecology and the Environment*, *5*, 365–374. https://doi.org/10.1890/1540-9295(2007)5[365:ANGOCE]2.0.CO;2

Jia, X., Dini-Andreote, F., & Salles, J. F. (2018). Community assembly processes of the microbial rare biosphere. *Trends in Microbiology*, *26*, 738–747. https://doi.org/10.1016/j.tim.2018.02.011

Jones, S. E., & Lennon, J. T. (2010). Dormancy contributes to the maintenance of microbial diversity. *Proceedings of the National Academy of Sciences of the United States of America*, *107*, 5881–5886. https://doi.org/10.1073/pnas.0912765107

Jousset, A., Bienhold, C., Chatzinotas, A., Gallien, L., Gobet, A., Kurm, V., Küsel, K., Rillig, M. C., Rivett, D. W., Salles, J. F., van Der Heijden, M. G., Youssef, N. H., Zhang, X., Wei, Z., & Hol, W. H. G. (2017). Where less may be more: How the rare biosphere pulls ecosystems strings. *The ISME Journal*, *11*, 853–862. https://doi.org/10.1038/ismej.2016.174

Kilibarda, M., Hengl, T., Heuvelink, G. B., Gräler, B., Pebesma, E., Perčec Tadić, M., & Bajat, B. (2014). Spatio-temporal interpolation of daily temperatures for global land areas at 1 km resolution. *Journal of Geophysical Research: Atmospheres*, *119*, 2294–2313. https://doi.org/10.1002/2013JD020803

Kirchman, D. L., Morán, X. A. G., & Ducklow, H. (2009). Microbial growth in the polar oceans–role of temperature and potential impact of climate change. *Nature Reviews Microbiology*, *7*, 451–459. https://doi.org/10.1038/nrmicro2115

Ladau, J., Shi, Y., Jing, X., He, J. S., Chen, L., Lin, X., Fierer, N., Gilbert, J. A., Pollard, K. S., & Chu, H. (2018). Existing climate change will lead to pronounced shifts in the diversity of soil prokaryotes. *mSystems*, *3*(5). https://doi.org/10.1128/mSystems.00167-18

Ledger, M. E., Edwards, F. K., Brown, L. E., Milner, A. M., & Woodward, G. U. Y. (2011). Impact of simulated drought on ecosystem biomass production: An experimental test in stream mesocosms. *Global Change Biology*, *17*, 2288–2297. https://doi.org/10.1111/j.1365-2486.2011.02420.x

Lennon, J. T., & Jones, S. E. (2011). Microbial seed banks: The ecological and evolutionary implications of dormancy. *Nature Reviews Microbiology*, *9*, 119–130. https://doi.org/10.1038/nrmicro2504

Li, Z., Tian, D., Wang, B., Wang, J., Wang, S., Chen, H. Y., Xu, X., Wang, C., He, N., & Niu, S. (2019). Microbes drive global soil nitrogen mineralization and availability. *Global Change Biology*, *25*, 1078–1088. https://doi.org/10.1111/gcb.14557

Liang, Y., Ning, D., Lu, Z., Zhang, N., Hale, L., Wu, L., Clark, I. M., McGrath, S. P., Storkey, J., Hirsch, P. R., Sun, B., & Zhou, J. (2020). Century long fertilization reduces stochasticity controlling grassland microbial community succession. *Soil Biology and Biochemistry*, *151*, 108023. https://doi.org/10.1016/j.soilbio.2020.108023

Lladó, S., López-Mondéjar, R., & Baldrian, P. (2017). Forest soil bacteria: Diversity, involvement in ecosystem processes, and response to global change. *Microbiology and Molecular Biology Reviews*, *81*(2). https://doi.org/10.1128/MMBR.00063-16

Lynch, M. D., & Neufeld, J. D. (2015). Ecology and exploration of the rare biosphere. *Nature Reviews Microbiology*, *13*, 217–229. https://doi.org/10.1038/nrmicro3400

Mariadassou, M., Pichon, S., & Ebert, D. (2015). Microbial ecosystems are dominated by specialist taxa. *Ecology Letters*, *18*, 974–982. https://doi.org/10.1111/ele.12478

Martiny, J. B., Martiny, A. C., Weihe, C., Lu, Y., Berlemont, R., Brodie, E. L., Goulden, M. L., Treseder, K. K., & Allison, S. D. (2017). Microbial legacies alter decomposition in response to simulated global change. *The ISME Journal*, *11*, 490–499. https://doi.org/10.1038/ismej.2016.122

Mirarab, S., Nguyen, N., Guo, S., Wang, L. S., Kim, J., & Warnow, T. (2015). PASTA: Ultra-large multiple sequence alignment for nucleotide and amino-acid sequences. *Journal of Computational Biology*, *22*, 377–386. https://doi.org/10.1089/cmb.2014.0156

Nemergut, D. R., Schmidt, S. K., Fukami, T., O'Neill, S. P., Bilinski, T. M., Stanish, L. F., Knelman, J. E., Darcy, J. L., Lynch, R. C., Wickey, P., & Ferrenberg, S. (2013). Patterns and processes of microbial community assembly. *Microbiology and Molecular Biology Reviews*, *77*, 342–356. https://doi.org/10.1128/MMBR.00051-12

Nielsen, U. N., & Ball, B. A. (2015). Impacts of altered precipitation regimes on soil communities and biogeochemistry in arid and semi-arid ecosystems. *Global Change Biology*, *21*, 1407–1421. https://doi.org/10.1111/gcb.12789

Ning, D., Deng, Y., Tiedje, J. M., & Zhou, J. (2019). A general framework for quantitatively assessing ecological stochasticity. *Proceedings of* *the National Academy of Sciences of the United States of America*, *116*, 16892–16898. https://doi.org/10.1073/pnas.1904623116

Price, M. N., Dehal, P. S., & Arkin, A. P. (2010). FastTree 2-approximately maximum-likelihood trees for large alignments. *PLoS ONE*, *5*, e9490. https://doi.org/10.1371/journal.pone.0009490

Ren, C., Chen, J., Lu, X., Doughty, R., Zhao, F., Zhong, Z., Han, X., Yang, G., Feng, Y., & Ren, G. (2018). Responses of soil total microbial biomass and community compositions to rainfall reductions. *Soil Biology and Biochemistry*, *116*, 4–10. https://doi.org/10.1016/j.soilbio.2017.09.028

Rousk, J., Smith, A. R., & Jones, D. L. (2013). Investigating the long-term legacy of drought and warming on the soil microbial community across five European shrubland ecosystems. *Global Change Biology*, *19*, 3872–3884. https://doi.org/10.1111/gcb.12338

Screen, J. A., & Simmonds, I. (2014). Amplified mid-latitude planetary waves favour particular regional weather extremes. *Nature Climate Change*, *4*, 704–709. https://doi.org/10.1038/nclimate2271

Seneviratne, S. I., Nicholls, N., Easterling, D., Goodess, C. M., Kanae, S., Kossin, J., Luo, Y., Marengo, J., McInnes, K., Rahimi, M., Reichstein, M., Sorteberg, A., Vera, C., & Zhang, X. (2012). Changes in climate extremes and their impacts on the natural physical environment. In C. B. Field, V. Barros, T. F. Stocker, D. Qin, D. J. Dokken, K. L. Ebi, M. D. Mastrandrea, K. J. Mach, G. K. Plattner, S. K. Allen, M. Tignor, & P. M. Midgley (Eds.), *Managing the risks of extreme events and disasters to advance climate change adaptation. A special report of working groups I and II of the Intergovernmental Panel on Climate Change (IPCC SREX Report)* (pp. 109–230). Cambridge University Press.

Shade, A., Jones, S. E., Caporaso, J. G., Handelsman, J., Knight, R., Fierer, N., & Gilbert, J. A. (2014). Conditionally rare taxa disproportionately contribute to temporal changes in microbial diversity. *mBio*, *5*. https://doi.org/10.1128/mBio.01371-14

Shade, A., Peter, H., Allison, S. D., Baho, D., Berga, M., Bürgmann, H., Huber, D. H., Langenheder, S., Lennon, J. T., Martiny, J. B., Matulich, K. L., Schmidt, T. M., & Handelsman, J. (2012). Fundamentals of microbial community resistance and resilience. *Frontiers in Microbiology*, *3*, 417. https://doi.org/10.3389/fmicb.2012.00417

Sheik, C. S., Beasley, W. H., Elshahed, M. S., Zhou, X., Luo, Y., & Krumholz, L. R. (2011). Effect of warming and drought on grassland microbial communities. *The ISME Journal*, *5*, 1692–1700. https://doi.org/10.1038/ismej.2011.32

Slatyer, R. A., Hirst, M., & Sexton, J. P. (2013). Niche breadth predicts geographical range size: A general ecological pattern. *Ecology Letters*, *16*, 1104–1114. https://doi.org/10.1111/ele.12140

Stegen, J. C., Lin, X., Konopka, A. E., & Fredrickson, J. K. (2012). Stochastic and deterministic assembly processes in subsurface microbial communities. *The ISME Journal*, *6*, 1653–1664. https://doi.org/10.1038/ismej.2012.22

Stenseth, N. C., Mysterud, A., Ottersen, G., Hurrell, J. W., Chan, K. S., & Lima, M. (2002). Ecological effects of climate fluctuations. *Science*, *297*, 1292–1296. https://doi.org/10.1126/science.1071281

Thompson, R. M., Beardall, J., Beringer, J., Grace, M., & Sardina, P. (2013). Means and extremes: Building variability into community-level climate change experiments. *Ecology Letters*, *16*, 799–806. https://doi.org/10.1111/ele.12095

Vellend, M. (2010). Conceptual synthesis in community ecology. *The Quarterly Review of Biology*, *85*, 183–206. https://doi.org/10.1086/652373

Wang, P., Chen, Y., Sun, Y., Tan, S., Zhang, S., Wang, Z., Zhou, J., Zhang, G., Shu, W., Luo, C., & Kuang, J. (2019). Distinct biogeography of different fungal guilds and their associations with plant species richness in forest ecosystems. *Frontiers in Ecology and Evolution*, *7*, 216. https://doi.org/10.3389/fevo.2019.00216

Wang, Z. H., Fang, J. Y., Tang, Z. Y., & Lin, X. (2011). Patterns, determinants and models of woody plant diversity in China. *Proceedings of the Royal Society B: Biological Sciences*, *278*, 2122–2132. https://doi.org/10.1098/rspb.2010.1897

Wang, Z. H., Fang, J. Y., Tang, Z. Y., & Lin, X. (2012). Relative role of contemporary environment versus history in shaping diversity patterns of China's woody plants. *Ecography*, *35*, 1124–1133. https://doi.org/10.1111/j.1600-0587.2011.06781.x

Zhou, J., Deng, Y., Shen, L., Wen, C., Yan, Q., Ning, D., Qin, Y., Xue, K., Wu, L., He, Z., Voordeckers, J. W., Van Nostrand, J. D., Buzzard, V., Michaletz, S. T., Enquist, B. J., Weiser, M. D., Kaspari, M., Waide, R., Yang, Y., & Brown, J. H. (2016). Temperature mediates continental-scale diversity of microbes in forest soils. *Nature Communications*, *7*, 12083. https://doi.org/10.1038/ncomms12083

Zhou, J., Deng, Y., Zhang, P., Xue, K., Liang, Y., Van Nostrand, J. D., Yang, Y., He, Z., Wu, L., Stahl, D. A., Hazen, T. C., Tiedje, J. M., & Arkin, A. P. (2014). Stochasticity, succession, and environmental perturbations in a fluidic ecosystem. *Proceedings of the National Academy of Sciences of the United States of America*, *111*, E836–E845. https://doi.org/10.1073/pnas.1324044111

Zhou, J., & Ning, D. (2017). Stochastic community assembly: Does it matter in microbial ecology? *Microbiology and Molecular Biology Reviews*, *81*, e00002–e00017. https://doi.org/10.1128/MMBR.00002-17

SUPPORTING INFORMATION

Additional supporting information may be found online in the Supporting Information section.

How to cite this article: Kuang, J., Bates, C. T., Wan, X., Ning, D., Deng, D., Shu, W., & Zhou, J. (2021). High historical variability weakens the effects of current climate differentiation on microbial community dissimilarity and assembly. *Global Change Biology*, 27, 5963–5975. https://doi.org/10.1111/gcb.15848